

Article type : Original Article

## Interplay between cytochrome *c* and gibberellins during *Arabidopsis* vegetative development

Sofía Racca<sup>1</sup>, Elina Welchen<sup>1</sup>, Diana E. Gras<sup>1</sup>, Danuše Tarkowská<sup>2</sup>, Veronika Turečková<sup>2</sup>, Veronica G. Maurino<sup>3</sup> and Daniel H. Gonzalez<sup>1,\*</sup>

<sup>1</sup>Instituto de Agrobiotecnología del Litoral (CONICET-UNL), Cátedra de Biología Celular y Molecular, Facultad de Bioquímica y Ciencias Biológicas, Universidad Nacional del Litoral, 3000 Santa Fe, Argentina,

<sup>2</sup>Laboratory of Growth Regulators, Centre of the Region Haná for Biotechnological and Agricultural Research, Institute of Experimental Botany AS CR, Faculty of Science, Palacký University, Šlechtitelů 27, CZ-78371 Olomouc, Czechia, and

<sup>3</sup>Institute of Developmental and Molecular Biology of Plants, Plant Molecular Physiology and Biotechnology Group, Heinrich-Heine-Universität, Universitätsstraße 1, and Cluster of Excellence on Plant Sciences (CEPLAS), 40225 Düsseldorf, Germany

\*For correspondence (email: [dhgonza@fcb.unl.edu.ar](mailto:dhgonza@fcb.unl.edu.ar))

**Correspondence to:** Daniel H. Gonzalez, Instituto de Agrobiotecnología del Litoral (CONICET-UNL), Centro Científico Tecnológico CONICET Santa Fe, Colectora Ruta Nac. 168 km 0, Paraje el Pozo s/n, 3000 Santa Fe, Argentina

Tel: +54 342 4511370 ext. 5016

E-mail: [dhgonza@fcb.unl.edu.ar](mailto:dhgonza@fcb.unl.edu.ar)

This article has been accepted for publication and undergone full peer review but has not been through the copyediting, typesetting, pagination and proofreading process, which may lead to differences between this version and the Version of Record. Please cite this article as doi: 10.1111/tpj.13845

This article is protected by copyright. All rights reserved.

**Running title:** Interplay between cytochrome *c* and gibberellins

**Keywords:** cytochrome *c*, gibberellin, DELLA protein, mitochondrion, *Arabidopsis thaliana*.

## SUMMARY

We studied the effect of reducing the levels of the mitochondrial electron carrier cytochrome *c* (CYTc) in *Arabidopsis thaliana*. Plants with CYTc deficiency have delayed growth and development, and reach flowering several days later than the wild-type but with the same number of leaves. CYTc-deficient plants accumulate starch and glucose during the day and contain lower levels of active gibberellins and higher levels of DELLA proteins, involved in gibberellin signaling. Gibberellin treatment abolishes the developmental delay and reduces glucose accumulation in CYTc-deficient plants, which also show a lower raise in ATP levels in response to glucose. Treatment of wild-type plants with inhibitors of mitochondrial energy production limits plant growth and increases the levels of DELLA proteins, thus mimicking the effects of CYTc deficiency. In addition, an increase in the amount of CYTc decreases DELLA protein levels and expedites growth, and this depends on active gibberellin synthesis. We conclude that CYTc levels impinge on the activity of the gibberellin pathway, most likely through changes in mitochondrial energy production. In this way, hormone-dependent growth would be coupled to the activity of components of the mitochondrial respiratory chain.

## INTRODUCTION

The mitochondrial respiratory chain is composed of several complexes that catalyze the transfer of electrons from succinate and reduced coenzymes to O<sub>2</sub> (Millar *et al.*, 2011). In addition to these complexes, two small electron carriers, ubiquinone and cytochrome *c* (CYTc), are required for

electron transfer to Complex III and between Complexes III and IV, respectively. CYTc is a small heme protein located in the mitochondrial intermembrane space (IMS). In addition to its role in respiration, CYTc acts in the import of proteins through the MIA40 pathway (Bihlmaier *et al.*, 2007), ascorbic acid synthesis (Bartoli *et al.*, 2000), D-lactate metabolism (Engqvist *et al.*, 2009; Welchen *et al.*, 2016) and programmed cell death (PCD; for reviews see Ow *et al.*, 2008; Welchen and Gonzalez, 2016). CYTc deficiency also affects the amount of respiratory complexes in several organisms, specifically of Complex IV in Arabidopsis (Welchen *et al.*, 2012).

The respiratory chain is more complex in plants than in other organisms. Oxidation of NADH can proceed not only through Complex I, but also through rotenone-insensitive NAD(P)H dehydrogenases located on the inner or the outer surface of the inner membrane (Rasmusson *et al.*, 2004). Like Complex I, these dehydrogenases are entry points to the respiratory chain. Unlike Complex I, however, they do not contribute to ATP synthesis. This also applies to the alternative oxidase (AOX) that accepts electrons from ubiquinone to reduce O<sub>2</sub>, thus bypassing Complexes III and IV (Van Aken *et al.*, 2009). This defines two different pathways, a cyanide-sensitive or CYTc-dependent pathway and a cyanide-insensitive or alternative pathway. The amount of energy produced by the oxidation of substrates will then strongly depend on the pathway of the electrons derived from these oxidation reactions.

The presence of an alternative pathway may help to cope with situations in which the cyanide-sensitive pathway is inhibited. As an example, flies expressing AOX are more resistant to cyanide and to defects in Complex IV (Fernandez-Ayala *et al.*, 2009). The cyanide-sensitive pathway is essential in plants since knockout of genes encoding CYTc causes embryo lethality (Welchen *et al.*, 2012). Dahan *et al.* (2014) were able to obtain plants that lack detectable Complex IV by *in vitro* cultivation of immature seeds. These plants have severe developmental alterations and apparently rely on an increased alternative respiratory activity.

The effect of partial loss of individual components of the cyanide-sensitive pathway in plants is less clear. Mitochondria from *Arabidopsis* mutants in *PPR40*, which encodes a pentatricopeptide repeat protein that associates with Complex III, show decreased cyanide-sensitive respiration, but normal Complex III levels. These plants are smaller than wild-type (WT) and hypersensitive to abscisic acid, salt and oxidative stress (Zsigmond *et al.*, 2008). Heterozygous *Arabidopsis* mutants in the heme *o* synthase gene *COX10* show about 50% decrease in Complex IV activity and early senescence (Mansilla *et al.*, 2015). In both cases, however, since the mutations do not directly affect structural components of the respiratory pathway, it is difficult to ascertain if the observed phenotypes are due to a decreased activity of the cyanide-sensitive pathway or to a specific role of the mutated gene. In the case of CYTc, *Arabidopsis* mutants with significantly reduced CYTc levels were isolated (Welchen *et al.*, 2012). Mitochondria from these mutants show increased cyanide-insensitive respiration and decreased Complex IV activity. In the present work, we further investigated the impact of decreasing CYTc levels in plants. We found that CYTc deficiency delays growth and development and causes carbohydrate accumulation, and that this is related to changes in gibberellin (GA) homeostasis. In addition, increasing CYTc levels expedites growth and development in a GA-dependent manner, suggesting that CYTc action is closely linked to GA metabolism.

## RESULTS

### **CYTc deficiency delays plant growth and development**

Single and double T-DNA insertion mutants in *CYTc-1* and *CYTc-2*, the genes encoding CYTc in *Arabidopsis*, were previously described (Welchen *et al.*, 2012). In this work, we analyzed two double mutant lines with considerably reduced CYTc levels due to the presence of T-DNA insertions in the 3'-UTR of *CYTc-1* (mutant *1b* in Figure S1) and either exon 1 or exon 3 of *CYTc-2* (mutants *2a* or *2b* in

Figure S1). We will refer to these lines as *cytc* mutants 1b2a and 1b2b throughout the paper. CYTc deficiency affects plant biomass, measured as either rosette fresh or dry weight. Three- and four-week-old *cytc* mutants grown under long-day (LD) photoperiod showed about 30-50% of the biomass of WT plants of the same age (Figure 1a). This difference was diminished and eventually lost after 5 weeks, mainly because the rosettes of WT plants stopped growing while those of mutants showed an extended growing period. Similar results, although over a longer time, were observed when plants were grown under short-day (SD) conditions (Figure S2). The decrease in rosette weight is the consequence of a decrease in both rosette size and the number of leaves of *cytc* mutants compared to WT plants of the same age (Figures 1a and S2). Since leaf number is associated to flowering, we measured the transition to reproductive development in WT and *cytc* mutants. Under both LD and SD conditions, the *cytc* mutants flowered several days later than WT plants (Figure 1b,c). However, when the number of leaves at flowering was measured, no difference was observed (Figure 1b,c). To analyze if the delay in flowering time could be related to differences at early developmental stages (i.e. seedling establishment), we measured the time required for the emergence of the first two leaves (stage 1.02 according to Boyes *et al.*, 2001). A delay of approximately 1 day in the appearance of the first two leaves was observed in *cytc* mutants relative to WT plants (Figure 1b,c). These results indicate that CYTc deficiency affects both seedling establishment and the duration of the vegetative phase.

We also analyzed the growth of single *cytc* mutants. Mutant 1b showed delayed growth while both mutants in *CYTc-2* showed no difference with WT (Figure S3a). An independent knockout mutant in *CYTc-1* (1a; Figure S1) also showed retarded growth (Figure S3b). This suggests that the developmental delay observed in the double mutants is mainly due to defects in *CYTc-1*. However, the double mutants showed a more pronounced phenotype and were used for subsequent studies.

## CYTc deficiency causes increased starch accumulation

We analyzed metabolite levels 1 h before (end of the night, ZT23) and 1 h after (beginning of the day, ZT1) the start of the illumination period in rosettes of *cytc* mutants grown under SD conditions (Table S1). Glucose and fructose levels were twice those of WT plants in both *cytc* mutant lines at ZT1 (Figure 2a). Statistically significant changes were also observed for other metabolites, such as increases in lysine and aspartic acid at ZT23 and in fumarate, phenylalanine and hydrophobic amino acids (isoleucine, leucine and valine) at ZT1 (Figure 2a). No significant differences in sucrose levels were observed (Table S1). Increased glucose and fructose levels led us to analyze the photosynthetic performance and starch accumulation. While photosynthetic parameters were not altered (Figure S4), we found that *cytc* mutants contained higher starch levels than WT plants (Figure 2c).

Quantification of starch levels at different times of the illumination period in plants of the same developmental stage (12 leaves) grown under SD conditions indicated that higher starch levels were mainly due to an increased rate of starch accumulation during the day (Figure 3a, left panel). The starch content of the mutants at the beginning of the day were not significantly different from those of WT plants. The difference in starch content at the end of the night was more pronounced in plants grown under LD conditions (Figure 3a, middle panel). Due to the shorter night period in this condition, the starch reserves in the mutants were not exhausted during the night.

To evaluate starch degradation independently of the preceding day/night cycles, we grew plants under continuous light and then transferred them to darkness. *cytc* mutants grown under continuous light also had higher starch content than WT plants (Figure 3a, right panel). In addition, starch degradation in the mutants took place at a higher rate than in the WT when the light was turned off (Figure 3a, right panel). We conclude that higher starch levels in *cytc* mutants are mainly the result of increased synthesis during the day. It is possible that the higher hexose levels observed after the onset of illumination triggered starch accumulation during the day. Indeed, glucose levels

in *cytc* mutants were higher than WT during the entire light period under SD and LD conditions (Figure 3b,c).

### **The expression of sugar-responsive genes is altered in *cytc* mutants**

Sugar levels regulate many aspects of plant physiology, including the expression of a large set of genes (Rolland *et al.*, 2006). High sugar levels promote the expression of genes involved in sugar utilization and reserve accumulation, while a decrease in sugar levels induces the expression of genes known as “starvation” genes. As *cytc* mutants have higher levels of soluble sugars, we analyzed the expression of the sugar-induced genes *APL3* and *MIPS1* (Villadsen and Smith, 2004; Usadel *et al.*, 2008) in plants of the same developmental stage. *APL3* and *MIPS1* transcript levels were higher in *cytc* mutants than in WT plants at ZT1 (Figure 3d). We further analyzed the expression of a set of sugar-repressed or “starvation” genes. These genes respond negatively to sugar levels and their expression is maximal at the end of the night when carbohydrate reserves are almost exhausted (Villadsen and Smith, 2004; Usadel *et al.*, 2008). Transcript levels of four of these genes (*ASN1*, *SEN1*, *SKIP20* and *ATL8*) were lower in the mutants than in the WT at ZT23 (Figure 3d). The observed changes in expression of these sugar-modulated genes agree with the fact that *cytc* mutants contain higher glucose levels than WT and indicate that the response of genes to sugar is not altered in the mutants.

### **Gibberellin treatment abolishes the developmental delay of *cytc* mutant plants**

The *cytc* mutants show increased carbohydrate accumulation and slow growth. Increased carbohydrate accumulation at the expense of growth was observed in plants that undergo carbon starvation episodes (Gibon *et al.*, 2004; Smith and Stitt, 2007). This response probably occurs to adjust growth to carbohydrate and/or energy availability and is due to a decrease in the levels of

bioactive GAs (Smith and Stitt, 2007; Paparelli *et al.*, 2013). We then analyzed the effect of GA treatment on the growth of *cytc* mutants. For this purpose, rosette biomass and rosette leaf number were measured after treating 10-day-old plants grown under LD conditions with 50  $\mu$ M GA<sub>4-7</sub>. GA treatment produced an increase in rosette leaf number relative to untreated plants of the same age in the mutants, but did not affect leaf number in WT plants (Figure 4a). As a consequence, the difference in rosette leaf number between WT plants and *cytc* mutants was progressively abolished after the treatment and *cytc* mutants flowered at the same time and with the same number of leaves as WT plants under this condition (Figure 4b-d). These results suggest that the developmental delay of *cytc* mutants may be associated to defects in GA homeostasis. Meanwhile, the differences in rosette size between WT plants and the mutants were maintained after the GA treatment (Figure S5).

To evaluate in more detail the changes in leaf production caused by GA, we analyzed WT and mutant plants grown under a 12 h light/12 h dark regime. Under these conditions, all plants have an extended vegetative period and flower with a higher number of leaves than plants grown under long days, thus allowing more accurate measurements. As observed under LD conditions, GA treatment caused a progressive increase in rosette leaf number in the mutants, compared with untreated plants (Figure S6). After 6 days of treatment (day 21 after sowing), the number of leaves of treated mutant plants was significantly higher than that of untreated mutant plants, but was still lower than the one of either treated or untreated WT plants (Figure S6). The differences between GA-treated mutant plants and WT plants were abolished after 9 days of treatment (Figure S6).

The GA treatment did not change the starch content in the mutants (Figure 4e). Glucose levels measured at ZT1, however, were significantly reduced by a single GA treatment performed two hours earlier (Figure 4f), suggesting that the observed increase in glucose levels is related to GA deficiency. In agreement with the observed decrease in glucose levels, a single GA treatment caused



a decrease in the expression of the glucose-induced gene *APL3* to levels similar to those of WT plants at ZT1 (Figure 4g).

### **CYTc deficiency alters GA homeostasis and the levels of DELLA proteins**

In view of the results obtained after GA treatment, we compared the levels of different endogenous GAs in WT and *cytc* mutant plants. Significant differences were observed for GA<sub>1</sub>, GA<sub>3</sub> and GA<sub>29</sub>, which showed lower levels in the mutants, and for GA<sub>15</sub>, which levels were higher (Figures 5a and S7). GA<sub>1</sub> and GA<sub>3</sub> are active GAs and this may explain why GA treatment rescues the developmental delay of *cytc* mutants. GA<sub>29</sub> is a catabolic product of GA<sub>20</sub>, a direct biosynthetic precursor of GA<sub>1</sub>. GA<sub>15</sub> belongs to a group of GA precursors (Hedden and Thomas, 2012). This suggests that the decrease in the levels of active GAs is probably due to reduced synthesis from metabolic intermediates and not to enhanced catabolism. In addition, we measured the levels of abscisic acid (ABA), which is antagonistic to GAs in several processes (Razem *et al.*, 2006), and found no differences between WT and *cytc* mutant plants (Figure S7).

To further analyze GA responses in *cytc* mutants, we measured the expression of GA-responsive genes. *GA20ox* and *GA3ox* genes encode enzymes involved in GA biosynthesis and are subjected to negative feedback regulation by GAs (Rieu *et al.*, 2008; Hedden and Thomas, 2012; Middleton *et al.*, 2012). We observed an induction of *GA20ox1*, *GA20ox2*, *GA20ox3* and *GA3ox1* in *cytc* mutants in comparison with WT plants either at ZT1 or ZT23 (Figure 5b). We also measured the expression of two genes induced by GAs: *GA2ox1*, involved in GA catabolism (Thomas *et al.*, 1999), and *GASA4* (Aubert *et al.*, 1998). Transcript levels of both genes were lower in *cytc* mutants than in WT plants (Figure 5c). The differences in expression of GA-responsive genes between WT and *cytc* mutant plants at ZT1 were abolished in most cases after a single GA treatment performed two hours earlier

(Figure 5d). The expression data are then consistent with the hypothesis that *cytc* mutants show defects in GA homeostasis.

GA action depends on DELLA proteins, which act as inhibitors of GA responses (Figure 5e; Sun, 2010). Upon binding to their receptors, GAs trigger DELLA proteins degradation. As DELLA protein levels are commonly used to monitor GA metabolism (Dill *et al.*, 2001; Griffiths *et al.*, 2006; Achard *et al.*, 2007), we analyzed the levels of the DELLA protein RGA *in vivo* using plants that express a fusion of RGA to GFP under the control of the *RGA* promoter (*pRGA:GFP-RGA*; Silverstone *et al.*, 2001). We crossed a line expressing this fusion to *cytc* mutant 1b (Figure S1) and then analyzed GFP-RGA fluorescence in homozygous plants (Figure 6a-d). Consistent with previous observations (Achard *et al.*, 2007), GFP-RGA nuclear fluorescence was detected in WT plants grown under illumination shortly after the light was turned off (Figure 6b) but the signal was barely detectable after prolonged incubation in darkness (Figure 6d). In the case of *cytc* mutant plants, increased nuclear fluorescence, indicative of higher GFP-RGA levels, was consistently observed under both conditions (Figure 6a,c). Quantification of the images obtained from 20 plants of each genotype indicated that both the number of nuclei with detectable fluorescence over background and the fluorescence intensity of these nuclei were higher in the *cytc* mutant than in WT plants (Figure 6e). We also analyzed RGA protein levels in WT and *cytc* mutant plants using specific antibodies. Western blot analysis indicated that RGA levels were higher in *cytc* mutants than in WT plants (Figure 6f). This is probably due to increased stability of the protein, since transcript levels of the *RGA* gene were lower in the mutants than in WT plants (see below). The level of RGL3, another DELLA protein, was also higher in *cytc* mutants (Figure 6f).

Starvation directly impacts on GA biosynthesis through changes in expression of the gene that encodes the GA biosynthetic enzyme *ent*-kaurene synthase (*KS*), which is repressed under this condition (Paparelli *et al.*, 2013). Expression of *KS* was higher in *cytc* mutants than in WT plants at ZT1 and ZT23 (Figure S8), suggesting that a different mechanism operates in this case. In addition,

transcript levels of *KO* and *KAO* genes, which encode enzymes involved in other steps of the GA synthesis pathway (*ent*-kaurene oxidase and *ent*-kaurenoic acid oxidase; Hedden and Thomas, 2012), were similar to those of WT plants (Figure S8). Considering that Paparelli *et al.* (2013) observed repression of the *KS* gene at the time of its maximal daily expression (ZT8), we also analyzed expression of this gene at ZT8 in *cytc* mutants. No differences between WT and *cytc* mutants were observed (Figure S9). Changes in expression of *GA20ox1*, *GA3ox1* and *GA2ox1* at ZT8 were similar to those observed at ZT1 (Figure S9).

We also measured the expression of genes that encode components of the GA signaling pathway (Figure S10). We observed increased expression of *GID1a* and *GID1b*, encoding two isoforms of the Arabidopsis GA receptor (Griffiths *et al.*, 2006), and of *SLY1* and *SLY2*, that participate in DELLA protein degradation (McGinnis *et al.*, 2003; Ariizumi *et al.*, 2011), at ZT1 (Figure S10). Since most of these genes are subjected to negative feedback regulation by GA through the action of DELLA proteins (Hedden and Thomas, 2012; Ribeiro *et al.*, 2012), their increased expression in *cytc* mutants is probably due to increased amounts of DELLA proteins. In contrast, transcript levels of the *RGA* gene were reduced in *cytc* mutants (Figure S10). Since *RGA* is induced by GA (Silverstone *et al.*, 1998), the reduced expression may be due to decreased GA signaling in *cytc* mutants. In summary, the observed expression changes seem to be the consequence, rather than the cause, of defective GA homeostasis in *cytc* mutants.

### **Inhibition of mitochondrial energy production mimics the effect of CYTc deficiency on growth and GA homeostasis**

To explore in more detail the link between CYTc levels and GA homeostasis, we analyzed hypocotyl growth, a process in which GA plays an important role (Cowling and Harberd, 1999). For this purpose, plants were grown during 4 days under long-day conditions and then incubated in the

presence of glucose, which promotes hypocotyl elongation, during 3 additional days. As shown in Figure 7a, *cytc* mutant plants showed reduced hypocotyl elongation. Treatment with GA promoted growth, both in mutants and in WT plants, but the relative response to the hormone was higher in the mutants (Figure 7b). This suggests that defective GA homeostasis is one of the factors that limit growth in these plants. In agreement with this, treatment of WT plants with the GA biosynthesis inhibitor paclobutrazol mimicked the effect of CYTc deficiency, while hypocotyl elongation in the mutant was barely affected (Figure 7c). We then asked if the growth defect observed in *cytc* mutants may be related to its participation as an electron carrier in the respiratory chain. Treatment of WT plants with the Complex III inhibitor Antimycin A (AA) caused a dose-dependent inhibition of hypocotyl growth (Figure 7d), indicating that CYTc-dependent respiration is required for growth. Notably, no significant inhibition was observed with 1  $\mu$ M AA in *cytc* mutant plants, which showed similar growth than WT plants in the presence of this and higher AA concentrations (Figure 7d). Thus, inhibition of CYTc-dependent respiration in WT plants mimics the effect of CYTc deficiency. In addition, growth inhibition by 1  $\mu$ M AA was reversed by GA (Figure 7e), suggesting that defective GA homeostasis is at least partially responsible for the effect of AA on growth. In agreement with this, AA treatment caused an increase in the levels of the DELLA protein RGA (Figure 7f). Treatment with the uncoupler 2,4-dinitrophenol (DNP) produced similar results as those observed with AA (Figure 7f-h), suggesting that the observed changes in GA homeostasis may be related to deficient energy production by the respiratory chain. Figure 7i shows that ATP levels significantly increased in hypocotyls of WT plants after glucose addition and this was blocked by AA. In *cytc* mutants, the raise in ATP levels was significantly lower than in WT plants (Figure 7i). The results suggest that deficient energy production is probably the cause of altered GA homeostasis.

### **Increased CYTc levels stimulate plant growth**

We expressed *CYTC-1* under the control of the *35SCaMV* promoter to produce plants with increased CYTc levels (Figure S11). These plants (*35S:CYTC*) showed increased rosette size, biomass and leaf number in comparison to WT plants of the same age (Figures 8a and S12a). *35S:CYTC* plants flowered with the same number of leaves but several days earlier than WT plants (Figure 8b,c and S12a). Similar observations were made when *CYTC-2*, instead of *CYTC-1*, was expressed under the control of the *35SCaMV* promoter (Figure S12b).

### **Active GA synthesis is required for the effect of increased CYTc levels on growth**

As the starch content was increased in the *cytc* mutants, we analyzed starch accumulation in *35S:CYTC* plants. Starch levels were similar in *35S:CYTC* and WT plants (Figure S13a). Glucose levels were also similar to WT in plants grown under SD conditions, while an increase was evident after the onset of illumination under LD conditions (Figure S13a). This difference disappeared at the end of the light cycle. Photosynthetic CO<sub>2</sub> fixation was also similar in *35S:CYTC* and WT plants (Figure S13b). These results suggest that an increase in CYTc levels does not modify carbon assimilation processes. Hence, it is possible that *35S:CYTC* plants make more efficient use of fixed carbon for growth. Total respiration (O<sub>2</sub> uptake) in *35S:CYTC* plants was also similar to WT (Figure S13c). However, respiration was more strongly inhibited in *35S:CYTC* plants after the addition of KCN (Figure S13c), suggesting a decreased capacity of the alternative pathway. Western blot analysis showed that AOX levels in *35S:CYTC* plants were similar to WT (Figure S13d), indicating that a decrease in AOX levels is not responsible for the observed changes in respiration. Complex IV activity levels were also similar in *35S:CYTC* and WT plants (Figure S13e).

Contrary to the observations made with the *cytc* mutants, RGA levels were lower in *35S:CYTC* plants than in WT plants, suggesting that GA signaling is activated in these plants (Figure 8d). To

analyze the requirement of GA for the effect of increased CYTc levels on plant growth, we crossed a *ga1-3* mutant line, defective in the initial step of GA biosynthesis (Tyler *et al.*, 2004), with a *35S:CYTc* line. Plants with increased CYTc levels in the *ga1-3* background (Figure 8e) were similar to *ga1-3* mutant plants, since they showed small rosettes and delayed flowering (Figure 8f, upper panel). This suggests that an active GA biosynthetic pathway is required for CYTc to affect growth. In agreement with this, treatment of *35S:CYTc* plants in the *ga1-3* background with GA resulted in plants similar to those with increased CYTc levels in a WT background (Figure 8f, lower panel).

## DISCUSSION

### **CYTc is required for optimal vegetative growth in Arabidopsis**

Plant mitochondria possess alternative pathways of respiration that can feed electrons from NADH to ubiquinone or deliver them from ubiquinone directly to O<sub>2</sub> (Millar *et al.*, 2011). Since they are not involved in proton translocation and ATP synthesis, these alternative pathways uncouple substrate oxidation from the energy status of the cell. They also allow substrate oxidation under conditions in which the canonical respiratory pathways, catalyzed by the rotenone-sensitive NADH dehydrogenase (Complex I) and the CYTc-dependent pathway, are blocked. The CYTc-dependent pathway is essential during embryogenesis, since knockout mutants in genes encoding CYTc, CYTc biogenesis or Complex IV biogenesis factors show embryo developmental arrest (Meyer *et al.*, 2005; Attallah *et al.*, 2011; Steinebrunner *et al.*, 2011; Welchen *et al.*, 2012; Mansilla *et al.*, 2015). Plants that lack detectable Complex IV activity, obtained by cultivation of immature seeds, have severe phenotypic alterations (Dahan *et al.*, 2014), showing the importance of CYTc-dependent respiration for post-germinative development. In a similar way, homozygous mutants in the Complex IV assembly factor gene *HCC1* rescued by expressing the *HCC1* cDNA from the embryo-specific *ABI3* promoter do not grow beyond the seedling stage (Steinebrunner *et al.*, 2014). The importance of

Complex I for post-germinative growth was also shown using knockout mutants in the gene that encodes the NDUFV1 subunit, which lack detectable Complex I activity (Kühn *et al.*, 2015). Although retarded in development, these mutants are able to survive if grown in the presence of sucrose before transferring them to soil. The results indicate that energy production by mitochondrial respiration is required during embryogenesis and early stages of plant development.

The role of mitochondrial energy producing pathways during vegetative development, when the photosynthetic apparatus is established, is less clear. Plants with significantly reduced amounts of Complex I show smaller rosettes and developmental delay (Meyer *et al.*, 2009; Pétriacq *et al.*, 2017). In these plants, not only seedling establishment, but also the duration of the vegetative phase, from seedling establishment to flowering, is affected. The same is true for plants with reduced amounts of CYTc, as described here, suggesting that the integrity of the energy-producing respiratory pathway from NADH to O<sub>2</sub> is required for optimal vegetative development.

#### **A deficiency in CYTc shifts carbon assimilation towards starch accumulation**

A salient feature of CYTc deficiency is increased starch accumulation due to increased synthesis during the light period. There is a negative correlation of rosette biomass with the amount of starch in leaves, reflecting a competition between growth and reserve accumulation (Cross *et al.*, 2006). In addition, optimal growth is achieved when the daily pattern of starch accumulation and use allows a continuous supply of carbohydrates to avoid starvation episodes (Gibon *et al.*, 2004; Smith and Stitt, 2007). If starvation occurs, a growth arrest signal is generated and a higher proportion of fixed carbon is used to increase reserves and avoid starvation during the following days. Delayed growth and increased starch content is also observed in *cytc* mutant plants. However, we did not detect symptoms of sugar starvation, since glucose levels were higher than in WT and “starvation” genes were repressed in these plants. We hypothesize that delayed growth and starch accumulation in the

*cytc* mutants are related to energy limitation due to changes in respiratory metabolism and not to carbon starvation.

#### **A decrease in the level of CYTc affects GA homeostasis**

Several lines of evidence indicate that GA homeostasis is affected in *cytc* mutants. We observed reduced levels of two active GAs, reduced expression of GA-induced genes and increased expression of GA-repressed genes. We also observed that GA treatment abolished the delay in development and the differences in expression of GA-responsive genes. Moreover, CYTc-deficient plants showed increased levels of the DELLA proteins RGA and RGL3, whose degradation is triggered by GA. Finally, the fact that GA treatment caused a decrease in glucose levels in the mutants but not in the WT, with the concomitant change in expression of the sugar-responsive gene *APL3*, suggests that defects in GA homeostasis are the cause of the increased glucose accumulation observed in *cytc* mutants.

#### **Inhibition of mitochondrial energy metabolism mimics the effects of CYTc deficiency**

In agreement with the notion that mitochondrial ATP synthesis is required for growth, treatment of plants with the Complex III inhibitor AA or the uncoupler DNP caused growth inhibition. At relatively low inhibitor levels, however, growth inhibition was reversed by GAs, suggesting that energy *per se* is not the main limiting factor under these conditions. It is tempting to speculate that decreased energy production by mitochondrial oxidative phosphorylation affects GA homeostasis so as to limit plant growth before energy reserves are exhausted. In agreement with this, AA and DNP treatments caused an increase in DELLA protein levels, as observed in CYTc-deficient plants. The fact that low inhibitor concentrations affected WT growth but had a minor effect on *cytc* mutants suggests that growth inhibition in the mutants is related to the function of CYTc in energy metabolism. Altogether,



our results indicate that CYTc deficiency affects growth through a decrease in energy production, which in turn affects GA homeostasis and DELLA protein levels.

In addition to its canonical role in respiratory metabolism, CYTc also participates in other processes, like MIA40-dependent protein import (Bihlmaier *et al.*, 2007), ascorbic acid synthesis (Bartoli *et al.*, 2000) and PCD (Ow *et al.*, 2008). Recently, MIA40 was connected to GA metabolism during seed germination (Uhrig *et al.*, 2017). Thus, one possibility would be that impairment of MIA40 function in *cytc* mutants is the cause of changes in GA homeostasis. MIA40, however, has been proposed as a negative regulator of GA-related processes (Uhrig *et al.*, 2017), which is opposite to our findings for CYTc. In addition, Complex I and Cu/Zn-SOD levels, which are affected by MIA40 deficiency (Carrie *et al.*, 2010), are normal in the *cytc* mutants under study (Welchen *et al.*, 2012). This, and the fact that inhibition of Complex III and uncoupling of respiration and energy production, which would not affect the delivery of electrons from MIA40 to CYTc, mimic the effects of CYTc deficiency, indicate that defective GA homeostasis in *cytc* mutants is not related to MIA40 function. The *cytc* mutants under study also have normal ascorbic acid levels (Welchen *et al.*, 2012), suggesting that deficiencies in ascorbic acid metabolism are not responsible for the observed effects of CYTc deficiency. If any, the role of CYTc in PCD in plants, unlike the situation in animals, is far from being understood (Daneva *et al.*, 2016). Although an effect of defective PCD on growth and GA homeostasis in *cytc* mutants cannot be completely ruled out, current evidence indicates that developmental PCD is required for the differentiation of specific cell types, rather than for generalized plant growth (Daneva *et al.*, 2016). Thus, in view of our results and the existing literature we favor the hypothesis that altered GA homeostasis and defective growth in *cytc* mutants are due to the role of CYTc in energy metabolism. The fact that GA treatment ameliorates the growth of mutants in subunits of Complex I (Pellny *et al.*, 2008; Meyer *et al.*, 2009) also supports the existence of a link between mitochondrial energy metabolism and GA homeostasis. Energy sensors, like Target of Rapamycin (TOR) or SNF1-related protein kinase1 (SnRK1) (Baena-González and Hanson, 2017), are likely candidates as mediators between mitochondrial energy production and GA homeostasis.

This article is protected by copyright. All rights reserved.

The fact that the transcriptional changes observed in *cytc* mutants for genes involved in GA metabolism and signaling seem to be the consequence, rather than the cause, of altered GA homeostasis suggests that post-translational modifications of GA synthesis or signaling components may be involved. Further studies are required to evaluate this.

### **CYTc is a limiting factor for Arabidopsis growth**

It is interesting that not only defects in CYTc affect plant growth, but also increased CYTc levels promote expedited growth. An increase in CYTc reduces DELLA protein levels and active GA biosynthesis is required for the effect of increased CYTc on growth. This suggests the existence of a close link between CYTc, GAs and growth. The fact that increasing CYTc levels promotes expedited growth suggests that CYTc is a limiting factor for plant growth, at least in Arabidopsis. Since the effect of CYTc on growth is most likely related to its role in energy metabolism, this may imply that CYTc levels limit the activity of the cyanide-sensitive pathway in Arabidopsis. *35S:CYTC* plants showed a decrease in the capacity of the alternative pathway and no significant changes in total respiration. Whether this results in a higher respiratory flux through the cyanide-sensitive pathway *in vivo* cannot be answered at this point and will require additional studies, like the measurement of oxygen isotope fractionation in these plants.

### **Conclusions**

The results presented here indicate that CYTc levels influence GA homeostasis to modulate plant growth. Our study suggests that energy production linked to the activity of the CYTc-dependent pathway affects GA metabolism and the levels of DELLA proteins. Under CYTc deficiency, plant growth and development are delayed and carbohydrate levels increase. Treatments with GA indicate that this is not related to energy limitation *per se*, but to altered GA homeostasis. This reveals the

existence of a regulatory mechanism that links plant mitochondrial energy metabolism to hormonal regulation of growth. This mechanism probably emerged to adjust plant growth to the functioning of energy-producing pathways to avoid damage of cellular functions due to a shortage of energy supply. A scheme is emerging in which different aspects of carbon metabolism impact on hormone signaling pathways to couple plant development to the metabolic status of the plant. CYTc, possibly through its role as a component of the mitochondrial respiratory chain, can be considered as a regulator of plant growth, linking carbon utilization and hormonal pathways. As such, from a technological perspective, manipulation of CYTc levels may be useful to modulate plant growth and development.

## EXPERIMENTAL PROCEDURES

### Plant material and growth conditions

Plants used in this study were in the *Arabidopsis thaliana* ecotype Columbia (Col-0) background. Lines with T-DNA insertions in genes encoding CYTc (GK586B10 and SALK\_143142 in *CYTc-1*; SALK\_037790 and SALK\_029663 in *CYTc-2*; Figure S1) were described previously, as well as double mutants between SALK\_143142 (knock-down) and either of the *CYTc-2* knockout mutants (Welchen *et al.*, 2012). Double mutants with GK586B10 are not viable (Welchen *et al.*, 2012). *ga1-3* mutant plants were kindly provided by Dr. Stephen Thomas (Rothamsted Research, UK). *pRGA:GFP-RGA* plants were obtained from the Arabidopsis Biological Resource Center (Ohio State University, Columbus, OH, USA). Plants were grown in pots on white peat bedding substrate under either LD (16 h light/8 h dark) or SD (8 h light/16 h dark) photoperiods at an intensity of  $100 \mu\text{mol m}^{-2} \text{s}^{-1}$  and a temperature of 22-24°C. To analyze DELLA protein levels, plants were grown for 7 days in darkness in Petri dishes containing 0.5x MS medium. For GA treatments, 5  $\mu\text{l}$  of a 50  $\mu\text{M}$  solution of GA<sub>4-7</sub> dissolved with drops of methanol in distilled water-0.1% Tween 20 were applied every 2 days onto

the shoot apex. Control plants were treated with the same solution without hormone. The treatment was started when WT and mutant plants contained at least two visible leaves (see figure legends for specific details). For the analysis of gene expression and glucose levels, a single GA treatment was performed 1 h before the beginning of the light period on WT and mutant plants of the same developmental stage (12 leaves) grown under SD conditions. Rosette dry weight was obtained after incubation at 60°C until constant weight. To analyze the effect of inhibitors, plants were grown for 4 days in plates containing liquid 0.5x MS medium under long-day conditions and then treated with 100 mM glucose, mainly as described by Xiong *et al.* (2013). Treatments with AA, DNP, paclobutrazol and GA<sub>3</sub> were started at the time of glucose addition.

#### **Genetic constructs and plant transformation**

For expression of *CYTC-1* and *CYTC-2* from the *35SCaMV* promoter, the entire coding sequences of the respective cDNAs, including the stop codons, were amplified with specific primers (Table S2) and cloned into entry vector pENTR<sup>TM</sup>3C (Thermo Fisher Scientific). The inserts were then introduced into the pAUL1 binary vector (Lyska *et al.*, 2013) through Gateway cloning. Constructs were introduced into *Arabidopsis* by floral dip (Clough and Bent, 1998). Transformants were selected on the basis of glufosinate (Basta<sup>TM</sup>) resistance and analyzed. A line expressing *CYTC-1* in a *ga1-3* background was obtained by crossing *35S:CYTC* line 1 with the *ga1-3* mutant followed by self-pollination to obtain the double homozygous line.

#### **Gene expression analysis**

Transcript levels were measured by reverse transcription followed by quantitative PCR (RT-qPCR) of total RNA prepared from rosettes of plants at the same developmental stage (12 leaves) harvested at the times indicated in the respective figures. Samples were collected, frozen in liquid nitrogen and

Accepted Article  
stored at -80°C until use. Total RNA was prepared using TRIzol reagent followed by a LiCl precipitation step. Reverse transcription was performed on an aliquot of RNA (1.5-2.0 µg) using an oligo(dT)<sub>18</sub> primer and MMLV reverse transcriptase (Promega). qPCR was performed on an aliquot of the cDNA using specific primers for the gene of interest (Table S2) and SYBR Green detection in an MJ Research Chromo4 or a Stratagene MX3000 apparatus. C<sub>t</sub> values were normalized using values for *ACT2* and *ACT8* actin genes (Charrier *et al.*, 2002). Results are expressed as the mean±SD of three biological replicates.

### Confocal microscopy

GFP-RGA fluorescence was detected using a Leica TCS SP8 confocal microscope with excitation at 488 nm and detection at 498-531 nm for GFP and 612-759 nm for chlorophyll. Images, overlays and Z-stacks were acquired and processed using the ImageJ analysis software.

### Western blot analysis

Western blot analysis was performed on total protein extracts. Plant material was ground in a precooled mortar in the presence of liquid nitrogen. Then, 300 mg of homogenate were collected in an Eppendorf tube with 300 µl of 125 mM Tris-HCl (pH 8.8), 1% (w/v) SDS, 10% glycerol, 50 mM Na<sub>2</sub>S<sub>2</sub>O<sub>5</sub> and 0.2 mM PMSF. The tubes were warmed to room temperature to solubilize the SDS and centrifuged at maximum speed in a microfuge for 10 min. The supernatant was saved in a new tube with 1/10 of 125 mM Tris-HCl (pH 6.9), 12% (w/v) SDS, 15% (v/v) glycerol, 22% (v/v) β-mercaptoethanol and 0.001% (w/v) Bromophenol Blue. For analysis, 40 µg of protein were separated by SDS-PAGE and transferred to Hybond-ECL (GE Healthcare). Blots were hybridized with monoclonal antibodies prepared against pigeon CYTc (7H8.2C12, Pharmingen, San Diego, CA, USA) or polyclonal rabbit antibodies against RGA (Agrisera, Vännäs, Sweden; dilution 1:1000), RGL3

(Agrisera, dilution 1:1000), AOX (Agrisera, dilution 1:1000) or COX2 (prepared in-house; dilution 1:1000). Secondary antibodies conjugated with horseradish peroxidase (Agrisera anti-mouse and anti-rabbit IgG; dilution 1:1000 and 1:25000 respectively) and the SuperSignal West Pico Chemiluminescent Substrate (Thermo Fisher Scientific) were used for detection of the signal. BN-PAGE and Complex IV activity measurements were performed as described previously (Mansilla *et al.*, 2015).

### **Metabolite analysis**

For metabolite analysis rosettes of individual 4-week-old plants grown under SD were harvested at ZT1 and ZT23, shock frozen in liquid nitrogen as described by Liseč *et al.* (2006) and stored at -80°C until analysis. Ground material of 50-80 mg was extracted in methanol:chloroform:water (5:2:1) with ribitol for internal standardization as described by Lee and Fiehn (2008) and analyzed by gas chromatography-mass spectrometry (GC-MS) according to Fiehn and Kind (2007) using a 7890B GC coupled to a 7200 QTOF (Agilent Technologies, Santa Clara, CA, USA). Data analysis was conducted with the Mass Hunter Software (Agilent Technologies). For relative quantification, all metabolite peak areas were normalized to the peak area of the internal standard ribitol (Sigma-Aldrich, St. Louis, MO, USA) added prior to extraction. Starch and glucose levels were quantified in plants of the same developmental stage using the methods described in Smith and Zeeman (2006). Qualitative starch assays were performed with lugol staining. Rosettes of individual plants grown under SD conditions were harvested and boiled in 50 ml of 80% (v/v) ethanol and stained with a fresh iodine solution (5 g I<sub>2</sub> and 0.5 g KI in 500 ml of distilled water) for 1-2 h and photographed immediately. ATP levels were determined according to standard protocols using a Bioluminescent Assay Kit (Sigma-Aldrich).

## Determination of GA and ABA content

GA and ABA content were determined in rosettes of 4-week-old plants grown under SD harvested at the end of the day (ZT7). The sample preparation and analysis of GAs was performed according to the method described in Urbanová *et al.* (2013) with some modifications. Briefly, freeze-dried plant tissue samples of 10 mg were ground to a fine consistency using 3-mm zirconium oxide beads (Retsch GmbH & Co. KG, Haan, Germany) and a MM 301 vibration mill at a frequency of 30 Hz for 3 min (Retsch GmbH & Co. KG, Haan, Germany) with 1 ml of ice-cold 80% acetonitrile containing 5% formic acid as extraction solution. The samples were then extracted overnight at 4°C using a Stuart SB3 benchtop laboratory rotator (Bibby Scientific Ltd., Staffordshire, UK), after adding 17 internal GA standards ( $[^2\text{H}_2]\text{GA}_1$ ,  $[^2\text{H}_2]\text{GA}_3$ ,  $[^2\text{H}_2]\text{GA}_4$ ,  $[^2\text{H}_2]\text{GA}_5$ ,  $[^2\text{H}_2]\text{GA}_6$ ,  $[^2\text{H}_2]\text{GA}_7$ ,  $[^2\text{H}_2]\text{GA}_8$ ,  $[^2\text{H}_2]\text{GA}_9$ ,  $[^2\text{H}_2]\text{GA}_{15}$ ,  $[^2\text{H}_2]\text{GA}_{19}$ ,  $[^2\text{H}_2]\text{GA}_{20}$ ,  $[^2\text{H}_2]\text{GA}_{24}$ ,  $[^2\text{H}_2]\text{GA}_{29}$ ,  $[^2\text{H}_2]\text{GA}_{34}$ ,  $[^2\text{H}_2]\text{GA}_{44}$ ,  $[^2\text{H}_2]\text{GA}_{51}$  and  $[^2\text{H}_2]\text{GA}_{53}$ ; purchased from Professor Lewis Mander, Australian National University). The homogenates were centrifuged at 36 670 x *g* and 4°C for 10 min. Corresponding supernatants were further purified using reversed-phase and mixed mode SPE cartridges (Waters, Milford, MA, USA) and analyzed by ultra-high performance chromatography-tandem mass spectrometry (UHPLC-MS/MS; Micromass, Manchester, U.K). GAs were detected using multiple-reaction monitoring mode of the transition of the ion  $[\text{M}-\text{H}]^-$  to the appropriate product ion. Masslynx 4.1 software (Waters, Milford, MA, USA) was used to analyze the data and the standard isotope dilution method (Rittenberg and Foster, 1940) was used to quantify GA levels.

For the determination of ABA, the plant tissues (approximately 20 mg DW of each sample) were homogenized and extracted for 1 h in 1 ml ice-cold methanol/water/acetic acid (10/89/1 v/v). Deuterium-labelled standard (20 pmol of (+)-3',5',5',7',7',7'- $^2\text{H}_6$ -ABA) was added to each sample. The homogenates were centrifuged (20 000 x *g*, 10 min, 4°C) after extraction, and the pellets were then re-extracted in 0.5 ml extraction solvent for 30 min. The combined extracts were purified by solid-phase extraction on Oasis® HLB cartridges (60 mg, 3 ml, Waters, Milford, MA, USA), evaporated

to dryness in a Speed-Vac (UniEquip) and finally analysed by UPLC-ESI(-/+)-MS/MS (Turečková et al., 2009).

### Respiration measurements

Respiration measurements were performed according to Mansilla *et al.* (2015). Briefly, plants were kept in darkness for 40 min and then 4th, 5th and 6th leaves were transferred to 2.5 mL of reaction buffer (300 mM mannitol, 1% (w/v) BSA, 10 mM potassium phosphate pH 7.2, 10 mM KCl, 5 mM MgCl<sub>2</sub>). Measurements were made at 25°C using a Clark-type oxygen electrode (Hansatech, Norfolk, England). The capacity of the alternative pathway was determined as the O<sub>2</sub> uptake sensitive to 10 mM SHAM in the presence of 1 mM KCN.

### ACKNOWLEDGEMENTS

We gratefully acknowledge Dr. Stephen Thomas for the *ga1-3* mutant, Dagmar Lyska and Peter Westhoff for the pAUL1 vector, the Arabidopsis Biological Resource Center for seed stocks and Agrisera for sending us a sample of the RGL3 antibody. This work was supported by grants from ANPCyT (Agencia Nacional de Promoción Científica y Tecnológica, Argentina) to DHG, CONICET (Consejo Nacional de Investigaciones Científicas y Técnicas, Argentina) and Universidad Nacional del Litoral to EW, the Deutsche Forschungsgemeinschaft (FOR 1186 and EXC 1028) to VGM, and the Deutsche Akademische Austauschdienst (DAAD) and Ministerio de Ciencia, Tecnología e Innovación Productiva (MINCyT, Argentina) through a Cooperative research grant (DAAD-PROALAR) to DHG and VGM. DHG, DEG and EW are members of CONICET. SR is a CONICET fellow. Financial support from the Ministry of Education, Youth and Sport of the Czech Republic through the National Program of Sustainability (Grant No. LO 1204) is also gratefully acknowledged. The authors declare no conflict of interest.

This article is protected by copyright. All rights reserved.



## AUTHORS' CONTRIBUTIONS

EW and DHG designed the experiments. SR performed the experiments with contributions from EW and DEG. VGM designed and performed the metabolite analysis. DT and VT performed the determination of GA and ABA. All authors analyzed data. EW made the figures with contributions from SR and DEG. DHG wrote the manuscript. All authors contributed to writing and accepted the final version of the manuscript.

## SHORT SUPPORTING INFORMATION LEGENDS

**Figure S1.** Scheme of the insertional mutants used in this study.

**Figure S2.** Phenotypic analysis of *cytc* mutant plants grown under SD photoperiod.

**Figure S3.** Phenotypic analysis of single *cytc* mutants.

**Figure S4.** Photosynthetic parameters of *cytc* mutant plants.

**Figure S5.** Effect of GA treatment on rosette biomass in WT plants and *cytc* mutants.

**Figure S6.** Effect of GA on the number of leaves of WT and *1b2a cytc* mutant plants grown under 12 h light/12 h dark photoperiod..

**Figure S7.** GA and ABA levels in WT and *cytc* mutant plants.

**Figure S8.** Transcript levels of genes encoding enzymes involved in GA biosynthesis.

**Figure S9.** Transcript levels of genes encoding enzymes involved in GA metabolism at ZT8.

**Figure S10.** Transcript levels of genes involved in GA signaling.

**Figure S11.** Western blot analysis of CYTc levels in different *35S:CYTC* lines.

**Figure S12.** Growth characteristics of plants that express *CYTC* genes from the *35SCaMV* promoter.

**Figure S13.** Metabolic characteristics of *35S:CYTC* plants.

**Table S1.** Metabolite content of WT and *cytc* mutant plants.

**Table S2.** Oligonucleotides used in this study.

## REFERENCES

- Achard, P., Liao, L., Jiang, C., Desnos, T., Bartlett, J., Fu, X. and Harberd, N.P.** (2007) DELLAs contribute to plant photomorphogenesis. *Plant Physiol.* **143**, 1163-1172.
- Ariizumi, T., Lawrence, P.K. and Steber, C.M.** (2011) The role of two f-box proteins, SLEEPY1 and SNEEZY, in Arabidopsis gibberellin signaling. *Plant Physiol.* **155**, 765-775.
- Attallah, C.V., Welchen, E., Martin, A.P., Spinelli, S.V., Bonnard, G., Palatnik, J.F. and Gonzalez, D.H.** (2011) Plants contain two SCO proteins that are differentially involved in cytochrome c oxidase function and copper and redox homeostasis. *J. Exp. Bot.* **62**, 4281-4294.
- Aubert, D., Chevillard, M., Dorne, A.M., Arlaud, G. and Herzog, M.** (1998) Expression patterns of GASA genes in Arabidopsis thaliana: the GASA4 gene is up-regulated by gibberellins in meristematic regions. *Plant Mol. Biol.* **36**, 871-883.
- Baena-González, E. and Hanson, J.** (2017) Shaping plant development through the SnRK1–TOR metabolic regulators. *Curr. Opin. Plant Biol.* **35**, 152-157.
- Bartoli, C.G., Pastori, G.M. and Foyer, C.H.** (2000) Ascorbate biosynthesis in mitochondria is linked to the electron transport chain between complexes III and IV. *Plant Physiol.* **123**, 335-344.
- Bihlmaier, K., Mesecke, N., Terzyiska, N., Bien, M., Hell, K. and Herrmann, J.M.** (2007) The disulfide relay system of mitochondria is connected to the respiratory chain. *J. Cell Biol.* **179**, 389-395.

**Boyes, D.C., Zayed, A.M., Ascenzi, R., McCaskill, A.J., Hoffman, N.E., Davis, K.R. and Görlach, J.**

(2001) Growth stage-based phenotypic analysis of Arabidopsis: a model for high throughput functional genomics in plants. *Plant Cell* **13**, 1499-1510.

**Carrie, C., Giraud, E., Duncan, O., Xu, L., Wang, Y., Huang, S., Clifton, R., Murcha, M., Filipovska, A.,**

**Rackham, O., et al.** (2010) Conserved and novel functions for Arabidopsis thaliana MIA40 in assembly of proteins in mitochondria and peroxisomes. *J. Biol. Chem.* **285**, 36138-36148.

**Charrier, B., Champion, A., Henry, Y. and Kreis, M.** (2002) Expression profiling of the whole

Arabidopsis shaggy-like kinase multigene family by real-time reverse transcriptase-polymerase chain reaction. *Plant Physiol.* **130**, 577-590.

**Clough, S.J. and Bent, A.F.** (1998) Floral dip: a simplified method for Agrobacterium-mediated

transformation of Arabidopsis thaliana. *Plant J.* **16**, 735-743.

**Cowling, R.J. and Harberd, N.P.** (1999) Gibberellins control Arabidopsis hypocotyl growth via

regulation of cellular elongation. *J. Exp. Bot.* **50**, 1351-1357.

**Cross, J.M., von Korff, M., Altmann, T., Bartzetko, L., Sulpice, R., Gibon, Y., Palacios, N. and Stitt,**

**M.** (2006) Variation of enzyme activities and metabolite levels in 24 Arabidopsis accessions growing in carbon-limited conditions. *Plant Physiol.* **142**, 1574-1588.

**Dahan, J., Tcherkez, G., Macherel, D., Benamar, A., Belcram, K., Quadrado, M., Arnal, N. and**

**Mireau, H.** (2014) Disruption of the CYTOCHROME C OXIDASE DEFICIENT1 gene leads to cytochrome c oxidase depletion and reorchestrated respiratory metabolism in Arabidopsis. *Plant Physiol.* **166**, 1788-1802.

**Daneva, A., Gao, Z., Van Durme, M. and Nowack, M.K.** (2016) Functions and regulation of

programmed cell death in plant development. *Annu. Rev. Cell Dev. Biol.* **32**, 441-468.

**Dill, A., Jung, H.S. and Sun, T.P.** (2001) The DELLA motif is essential for gibberellin-induced degradation of RGA. *Proc. Natl. Acad. Sci. USA* **98**, 14162-14167.

**Engqvist, M., Drincovich, M.F., Flugge, U.I. and Maurino, V.G.** (2009) Two D-2-hydroxy-acid dehydrogenases in *Arabidopsis thaliana* with catalytic capacities to participate in the last reactions of the methylglyoxal and beta-oxidation pathways. *J. Biol. Chem.* **284**, 25026-25037.

**Fernandez-Ayala, D.J., Sanz, A., Vartiainen, S., Kemppainen, K.K., Babusiak, M., Mustalahti, E., Costa, R., Tuomela, T., Zeviani, M., Chung, J., et al.** (2009) Expression of the *Ciona* intestinalis alternative oxidase (AOX) in *Drosophila* complements defects in mitochondrial oxidative phosphorylation. *Cell Metab.* **9**, 449-460.

**Fiehn, O. and Kind, T.** (2007) Metabolite profiling in blood plasma. *Meth. Mol. Biol.* **358**, 3-17.

**Gibon, Y., Bläsing, O.E., Palacios-Rojas, N., Pankovic, D., Hendriks, J.H., Fisahn, J., Höhne, M., Günther, M. and Stitt, M.** (2004) Adjustment of diurnal starch turnover to short days: depletion of sugar during the night leads to a temporary inhibition of carbohydrate utilization, accumulation of sugars and post-translational activation of ADP-glucose pyrophosphorylase in the following light period. *Plant J.* **39**, 847-862.

**Griffiths, J., Murase, K., Rieu, I., Zentella, R., Zhang, Z.L., Powers, S.J., Gong, F., Phillips, A.L., Hedden, P., Sun, T.P., et al.** (2006) Genetic characterization and functional analysis of the GID1 gibberellin receptors in *Arabidopsis*. *Plant Cell* **18**, 3399-3414.

**Hedden, P. and Thomas, S.G.** (2012) Gibberellin biosynthesis and its regulation. *Biochem. J.* **444**, 11-25.

**Kühn, K., Obata, T., Feher, K., Bock, R., Fernie, A.R. and Meyer, E.H.** (2015) Complete mitochondrial Complex I deficiency induces an up-regulation of respiratory fluxes that is abolished by traces of functional Complex I. *Plant Physiol.* **168**, 1537-1549.

**Lee, D.Y. and Fiehn, O.** (2008) High quality metabolomic data for *Chlamydomonas reinhardtii*. *Plant Methods* **4**, 7.

**Lisec, J., Schauer, N., Kopka, J., Willmitzer, L. and Fernie, A.R.** (2006) Gas chromatography mass spectrometry-based metabolite profiling in plants. *Nat. Protoc.* **1**, 387-396.

**Lyska, D., Engelmann, K., Meierhoff, K. and Westhoff, P.** (2013) pAUL: a gateway-based vector system for adaptive expression and flexible tagging of proteins in *Arabidopsis*. *PLoS One* **8**, e53787.

**Mansilla, N., García, L., Gonzalez, D.H. and Welchen, E.** (2015) AtCOX10, a protein involved in haem o synthesis during cytochrome c oxidase biogenesis, is essential for plant embryogenesis and modulates the progression of senescence. *J. Exp. Bot.* **66**, 6761-6775.

**McGinnis, K.M., Thomas, S.G., Soule, J.D., Strader, L.C., Zale, J.M., Sun, T.P. and Steber, C.M.** (2003) The *Arabidopsis* SLEEPY1 gene encodes a putative F-box subunit of an SCF E3 ubiquitin ligase. *Plant Cell* **15**, 1120-1130.

**Meyer, E.H., Giegé, P., Gelhaye, E., Rayapuram, N., Ahuja, U., Thöny-Meyer, L., Grienenberger, J.M. and Bonnard, G.** (2005) AtCCMH, an essential component of the c-type cytochrome maturation pathway in *Arabidopsis* mitochondria, interacts with apocytochrome c. *Proc. Natl. Acad. Sci. USA* **102**, 16113-16118.

**Meyer, E.H., Tomaz, T., Carroll, A.J., Estavillo, G., Delannoy, E., Tanz, S.K., Small, I.D., Pogson, B.J. and Millar, A.H.** (2009) Remodeled respiration in *ndufs4* with low phosphorylation efficiency suppresses *Arabidopsis* germination and growth and alters control of metabolism at night. *Plant Physiol.* **151**, 603-619.

**Middleton, A.M., Úbeda-Tomás, S., Griffiths, J., Holman, T., Hedden, P., Thomas, S.G., Phillips, A.L., Holdsworth, M.J., Bennett, M.J., King, J.R., et al.** (2012) Mathematical modeling elucidates the

role of transcriptional feedback in gibberellin signaling. *Proc. Natl. Acad. Sci. USA* **109**, 7571-7576.

**Millar, A.H., Whelan, J., Soole, K.L. and Day, D.A.** (2011) Organization and regulation of mitochondrial respiration in plants. *Annu. Rev. Plant Biol.* **62**, 79-104.

**Ow, Y.L., Green, D.R., Hao, Z. and Mak, T.W.** (2008) Cytochrome c: functions beyond respiration. *Nat. Rev. Mol. Cell Biol.* **9**, 532-542.

**Paparelli, E., Parlanti, S., Gonzali, S., Novi, G., Mariotti, L., Ceccarelli, N., van Dongen, J.T., Kölling, K., Zeeman, S.C. and Perata, P.** (2013) Nighttime sugar starvation orchestrates gibberellin biosynthesis and plant growth in Arabidopsis. *Plant Cell* **25**, 3760-3769.

**Pellny, T.K., Van Aken, O., Dutilleul, C., Wolff, T., Groten, K., Bor, M., De Paepe, R., Reyss, A., Van Breusegem, F., Noctor, G., et al.** (2008) Mitochondrial respiratory pathways modulate nitrate sensing and nitrogen-dependent regulation of plant architecture in *Nicotiana sylvestris*. *Plant J.* **54**, 976-992.

**Pétriacq, P., de Bont, L., Genestout, L., Hao, J., Laureau, C., Florez-Sarasa, I., Rzigui, T., Queval, G., Gilard, F., Mauve, C., et al.** (2017) Photoperiod affects the phenotype of mitochondrial Complex I mutants. *Plant Physiol.* **173**, 434-455.

**Rasmusson, A.G., Soole, K.L. and Elthon, T.E.** (2004) Alternative NAD(P)H dehydrogenases of plant mitochondria. *Annu. Rev. Plant Biol.* **55**, 23-39.

**Razem, F.A., Baron, K. and Hill, R.D.** (2006) Turning on gibberellin and abscisic acid signaling. *Curr. Opin. Plant Biol.* **9**, 454-459.

**Ribeiro, D.M., Araújo, W.L., Fernie, A.R., Schippers, J.H. and Mueller-Roeber, B.** (2012) Transcriptome and metabolome effects triggered by gibberellins during rosette growth in Arabidopsis. *J. Exp. Bot.* **63**, 2769-2786.

- Rieu, I., Ruiz-Rivero, O., Fernandez-Garcia, N., Griffiths, J., Powers, S.J., Gong, F., Linhartova, T., Eriksson, S., Nilsson, O., Thomas, S.G., et al.** (2008) The gibberellin biosynthetic genes AtGA20ox1 and AtGA20ox2 act, partially redundantly, to promote growth and development throughout the Arabidopsis life cycle. *Plant J.* **53**, 488-504.
- Rittenberg, D. and Foster, G.L.** (1940) A new procedure for quantitative analysis by isotope dilution, with application to the determination of amino acids and fatty acids. *J. Biol. Chem.* **133**, 737-744.
- Rolland, F., Baena-Gonzalez, E. and Sheen, J.** (2006) Sugar sensing and signaling in plants: conserved and novel mechanisms. *Annu. Rev. Plant Biol.* **57**, 675-709.
- Silverstone, A.L., Ciampaglio, C.N. and Sun, T.** (1998) The Arabidopsis RGA gene encodes a transcriptional regulator repressing the gibberellin signal transduction pathway. *Plant Cell* **10**, 155-169.
- Silverstone, A.L., Jung, H.S., Dill, A., Kawaide, H., Kamiya, Y. and Sun, T.P.** (2001) Repressing a repressor: gibberellin-induced rapid reduction of the RGA protein in Arabidopsis. *Plant Cell* **13**, 1555-1566.
- Smith, A.M. and Stitt, M.** (2007) Coordination of carbon supply and plant growth. *Plant Cell Environ.* **30**, 1126-1149.
- Smith, A.M. and Zeeman, S.C.** (2006) Quantification of starch in plant tissues. *Nat. Protoc.* **1**, 1342-1345.
- Steinebrunner, I., Gey, U., Andres, M., Garcia, L. and Gonzalez, D.H.** (2014) Divergent functions of the Arabidopsis mitochondrial SCO proteins: HCC1 is essential for COX activity while HCC2 is involved in the UV-B stress response. *Front. Plant Sci.* **5**, 87.

**Steinebrunner, I., Landschreiber, M., Krause-Buchholz, U., Teichmann, J. and Rödel, G.** (2011)

HCC1, the Arabidopsis homologue of the yeast mitochondrial copper chaperone SCO1, is essential for embryonic development. *J. Exp. Bot.* **62**, 319-330.

**Sun, T.P.** (2010) Gibberellin-GID1-DELLA: a pivotal regulatory module for plant growth and development. *Plant Physiol.* **154**, 567-570.

**Thomas, S.G., Phillips, A.L. and Hedden, P.** (1999) Molecular cloning and functional expression of gibberellin 2- oxidases, multifunctional enzymes involved in gibberellin deactivation. *Proc. Natl. Acad. Sci. USA* **96**, 4698-4703.

**Turečková, V., Novák, O. and Strnad, M.** (2009) Profiling ABA metabolites in *Nicotiana tabacum* L. leaves by ultra-performance liquid chromatography-electrospray tandem mass spectrometry. *Talanta* **80**, 390-399.

**Tyler, L., Thomas, S.G., Hu, J., Dill, A., Alonso, J.M., Ecker, J.R. and Sun, T.P.** (2004) Della proteins and gibberellin-regulated seed germination and floral development in Arabidopsis. *Plant Physiol.* **135**, 1008-1019.

**Uhrig, R.G., Labandera, A.M., Tang, L.Y., Sieben, N.A., Goudreault, M., Yeung, E., Gingras, A.C., Samuel, M.A. and Moorhead, G.B.** (2017) Activation of mitochondrial protein phosphatase SLP2 by MIA40 regulates seed germination. *Plant Physiol.* **173**, 956-969.

**Urbanová, T., Tarkowská, D., Novák, O., Hedden, P. and Strnad, M.** (2013) Analysis of gibberellins as free acids by ultra performance liquid chromatography–tandem mass spectrometry. *Talanta* **112**, 85-94.

**Usadel, B., Bläsing, O.E., Gibon, Y., Retzlaff, K., Höhne, M., Günther, M. and Stitt, M.** (2008) Global transcript levels respond to small changes of the carbon status during progressive exhaustion of carbohydrates in Arabidopsis rosettes. *Plant Physiol.* **146**, 1834-1861.



**Van Aken, O., Giraud, E., Clifton, R. and Whelan, J.** (2009) Alternative oxidase: a target and regulator of stress responses. *Physiol. Plant.* **137**, 354-361.

**Villadsen, D. and Smith, S.M.** (2004) Identification of more than 200 glucose-responsive Arabidopsis genes none of which responds to 3-O-methylglucose or 6-deoxyglucose. *Plant Mol. Biol.* **55**, 467-477.

**Welchen, E. and Gonzalez, D.H.** (2016) Cytochrome *c*, a hub linking energy, redox, stress and signalling pathways in mitochondria and other cell compartments. *Physiol. Plant.* **157**, 310-321.

**Welchen, E., Hildebrandt, T.M., Lewejohann, D., Gonzalez, D.H. and Braun, H.P.** (2012) Lack of cytochrome *c* in Arabidopsis decreases stability of Complex IV and modifies redox metabolism without affecting Complexes I and III. *Biochim. Biophys. Acta* **1817**, 990-1001.

**Welchen, E., Schmitz, J., Fuchs, P., García, L., Wagner, S., Wienstroer, J., Schertl, P., Braun, H.P., Schwarzländer, M., Gonzalez, D.H. and Maurino, V.G.** (2016) D-lactate dehydrogenase links methylglyoxal degradation and electron transport through cytochrome *c*. *Plant Physiol.* **172**, 901-912.

**Xiong, Y., McCormack, M., Li, L., Hall, Q., Xiang, C. and Sheen, J.** (2013) Glc-TOR signalling leads transcriptome reprogramming and meristem activation. *Nature* **496**, 181-186.  
**Zsigmond, L., Rigó, G., Szarka, A., Székely, G., Otvös, K., Darula, Z., Medzihradszky, K.F., Koncz, C., Koncz, Z. and Szabados, L.** (2008) Arabidopsis PPR40 connects abiotic stress responses to mitochondrial electron transport. *Plant Physiol.* **146**, 1721-1737.

## FIGURE LEGENDS

**Figure 1.** *cytc* mutants show delayed rosette growth.

(a) Parameters related to rosette growth in plants grown under LD photoperiod.

(b,c) Number of days after sowing (DAS) required for flowering and number of leaves at flowering in plants grown under LD (b) or SD (c) photoperiods. The dotted portion of the bars represents the time required for emergence of the first two leaves (stage 1.02).

Black bars, WT plants; white bars, *cytc* mutant 1b2a; gray bars, *cytc* mutant 1b2b. The bars represent the mean±SD of 12 plants from each genotype. Asterisks indicate significant differences ( $P < 0.01$ ) with WT plants of the same age, according to LSD Fisher tests. Representative images are shown in the right panels.

**Figure 2.** *cytc* mutants accumulate more glucose and fructose at the beginning of the day.

(a) Levels of several metabolites 1 h before the end of the night (ZT23) or 1 h after the beginning of the day (ZT1) in rosettes of WT plants (black bars) and *cytc* mutants (white and gray bars). Values are relative to WT at ZT23. The bars represent the mean±SD of four biological replicates. Asterisks indicate significant differences ( $P < 0.01$ ) with WT plants at the same ZT (Student's *t* test). Only metabolites with significant changes in both *cytc* mutants are shown.

(b) Schematic representation of the results shown in (a).

(c) Histochemical staining of starch at the end of the day (ZT8) and ZT23 in plants grown under short-day conditions.

**Figure 3.** *cytc* mutants accumulate starch and glucose during the day.

(a) Starch accumulation patterns during the illumination period in WT plants and *cytc* mutants grown under SD (left panel) or LD (middle panel) photoperiod, and starch degradation pattern in plants grown under continuous illumination at different times after the light was turned off (right panel).

(b,c) Glucose content in plants grown under SD (b) or LD (c) photoperiod.

(d) Transcript levels of sugar-responsive genes in WT and *cytc* mutant plants grown under SD conditions 1 h before (ZT23) and 1 h after (ZT1) the beginning of the illumination period. The bars represent the mean $\pm$ SD of three biological replicates and different letters indicate significant differences in transcript levels at the same ZT ( $P < 0.05$ ; LSD Fisher test).

Plants of the same developmental stage were used in these experiments. In (a-c), asterisks indicate significant differences ( $P < 0.01$ ) of both mutants with WT plants (LSD Fisher test; three biological replicates).

**Figure 4.** GA treatment abrogates the developmental delay of *cytc* mutant plants.

(a) Number of leaves of WT plants and *cytc* mutants grown under LD photoperiod either treated or not treated with 50  $\mu$ M GA<sub>4-7</sub>. The GA treatment was started at day 10 after sowing (DAS) and applied every 2 days at the end of the day. Control plants were treated with the solution used to dissolve GA. Different letters indicate significant differences at the same day ( $P < 0.01$ ; LSD Fisher test;  $n = 12$ ).

(b) Representative images of control and GA-treated plants after flowering.

(c,d) Number of days after sowing required for flowering (c) and number of leaves at flowering (d). Different letters indicate significant differences.

(e) Starch content at the end of the day in WT plants and *cytc* mutants either treated (dark gray bars) or not treated (light gray bars) with GA. Samples were harvested after 10 days of treatment. The bars represent the mean $\pm$ SD of three biological replicates.

(f) Glucose levels measured 2 h after a single GA (dark gray bars) or control (light gray bars) treatment performed 1 h before the end of the night. Asterisks indicate significant differences with control plants.

(g) Transcript levels of the sugar-responsive gene *APL3* in plants treated as in (f). The bars represent the mean $\pm$ SD of three biological replicates. Asterisks indicate significant differences ( $P < 0.05$ ; LSD Fisher test) with WT plants under the same condition.

**Figure 5.** GA content and transcript levels of GA-responsive genes in *cytc* mutant plants.

(a) The levels of GA<sub>1</sub>, GA<sub>3</sub>, GA<sub>29</sub> and GA<sub>15</sub> in WT and *cytc* mutant plants.

(b,c) Transcript levels of GA-repressed (b) and GA-induced (c) genes in WT plants and *cytc* mutants either 1 h before or 1 h after the start of the illumination period.

(d) *GA2ox1*, *GA20ox1* and *GA3ox1* transcript levels 1 h after the start of the illumination period in plants either treated or not treated with 50  $\mu$ M GA<sub>4-7</sub> two hours earlier.

(e) Scheme of the GA biosynthesis and signaling pathway. Gray lines indicate regulation of gene expression by bioactive GAs (Hedden and Thomas, 2012). Pointed and blunt arrows indicate positive and negative regulation, respectively.

Plants of the same developmental stage were used for these experiments. The bars represent the mean $\pm$ SD of five (a) or three (b-d) biological replicates. Different letters indicate significant differences ( $P < 0.05$ ; LSD Fisher Test).

**Figure 6.** *cytc* mutants contain higher levels of DELLA proteins.

(a-d) Confocal microscopy images of plants expressing *pRGA:GFP-RGA* in *cytc-1b* (a,c) of WT (b,d) background. The upper region of hypocotyls of plants grown under short-day conditions and transferred to darkness either for 1 h (a,b) or 16 h (c,d) was analyzed. The images show Z-stacks of seven optical longitudinal sections along a distance of 20  $\mu\text{m}$ . Nuclear GFP fluorescence is shown in green (arrows); chlorophyll autofluorescence is shown in red; yellow nuclei arise from the superimposition of regions with GFP and chlorophyll fluorescence in different sections. Representative images of 20 plants of each genotype in two independent experiments are shown. Scale bars: 50  $\mu\text{m}$ .

(e) Quantification of the number of nuclei with GFP fluorescence and the nuclear fluorescence intensity in the plants shown in (a) and (b). The bars represent the mean $\pm$ SD of 20 plants for each genotype. Different letters indicate significant differences ( $P < 0.05$ ; LSD Fisher Test).

(f) Western blot analysis of RGA and RGL3 protein levels in WT plants and *cytc* mutants. A sample of WT plants treated with the inhibitor of GA biosynthesis paclobutrazol (PAC) was included in the analysis. The experiment was repeated three times with similar results.

**Figure 7.** Inhibitors of mitochondrial energy metabolism mimic the effect of CYTc deficiency.

(a) Hypocotyl length of WT and *cytc* mutant plants in the presence of different  $\text{GA}_3$  concentrations.

(b) Effect of GA on hypocotyl growth in WT and *cytc* mutant plants. Values are expressed relative to controls without GA.

(c) Hypocotyl growth in WT and *cytc* mutant plants in the presence of different concentrations of the GA synthesis inhibitor paclobutrazol.

- (d) Hypocotyl growth in WT and *cytc* mutant plants in the presence of different AA concentrations.
- (e) The combined effect of AA and GA on hypocotyl growth in WT and *cytc* mutant plants. Plants were treated with either 1  $\mu$ M AA and/or 10  $\mu$ M GA<sub>3</sub>, as indicated.
- (f) Effect of inhibitors of mitochondrial energy production on the levels of the DELLA protein RGA. Plants expressing GFP-RGA were treated with glucose and either 25  $\mu$ M AA or 50  $\mu$ M DNP during 3 h. GFP fluorescence intensity was quantified in nuclei of treated and non-treated plants.
- (g) Hypocotyl growth in WT and *cytc* mutant plants in the presence of different DNP concentrations.
- (h) The combined effect of DNP and GA on hypocotyl growth in WT and *cytc* mutant plants. Plants were treated with either 25  $\mu$ M DNP and/or 10  $\mu$ M GA<sub>3</sub>, as indicated.
- (i) ATP levels in WT and *cytc* mutant plants after 3 h of incubation in the presence of 100 mM glucose either in the absence or presence of 25  $\mu$ M AA or 50  $\mu$ M DNP.

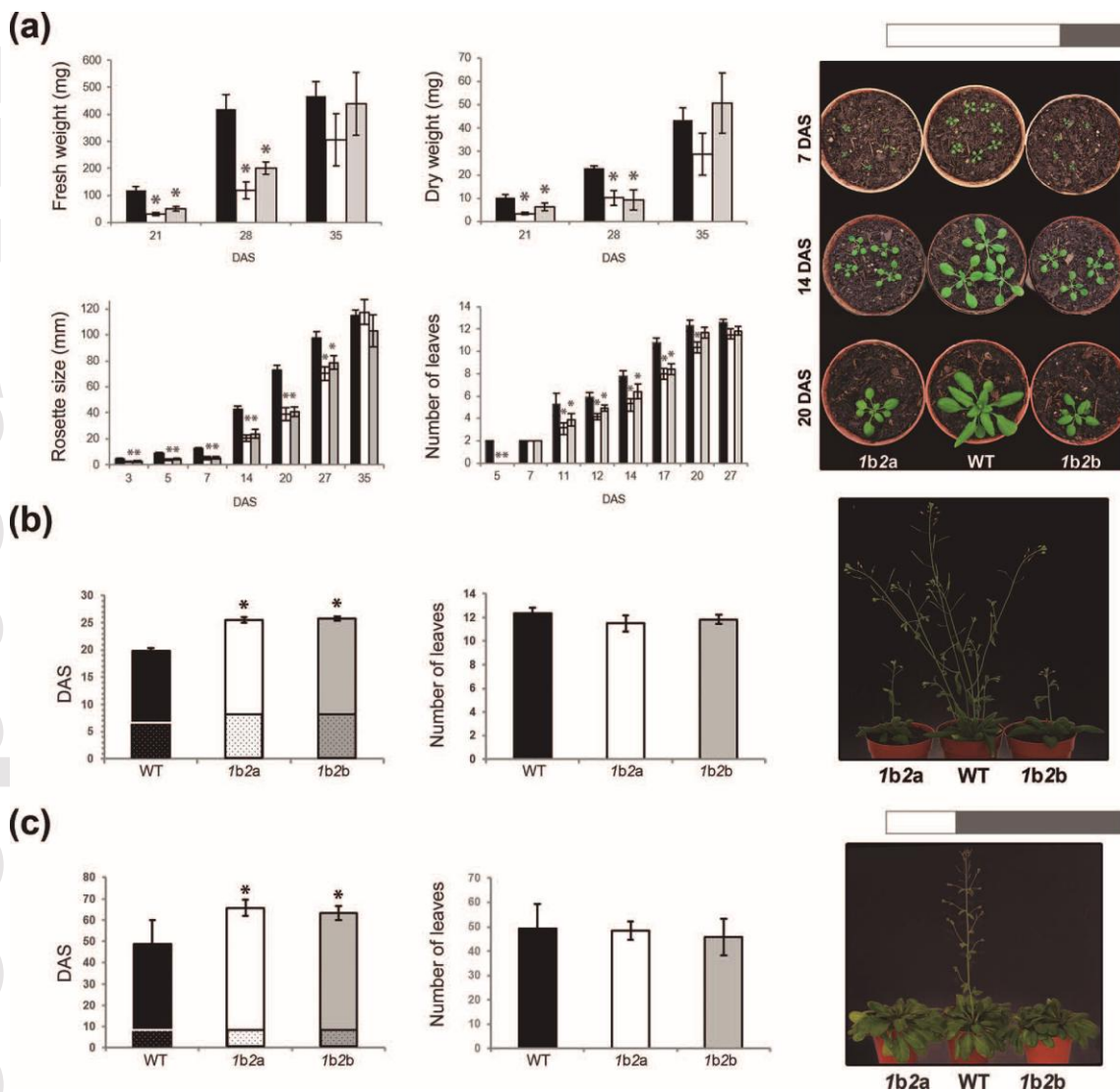
The bars represent the mean $\pm$ SE of 15-30 plants for each genotype and condition. Different letters indicate significant differences ( $P < 0.05$ ; ANOVA; Tukey HSD Test).

**Figure 8.** Increasing CYTc levels promotes expedited growth in a GA-dependent manner.

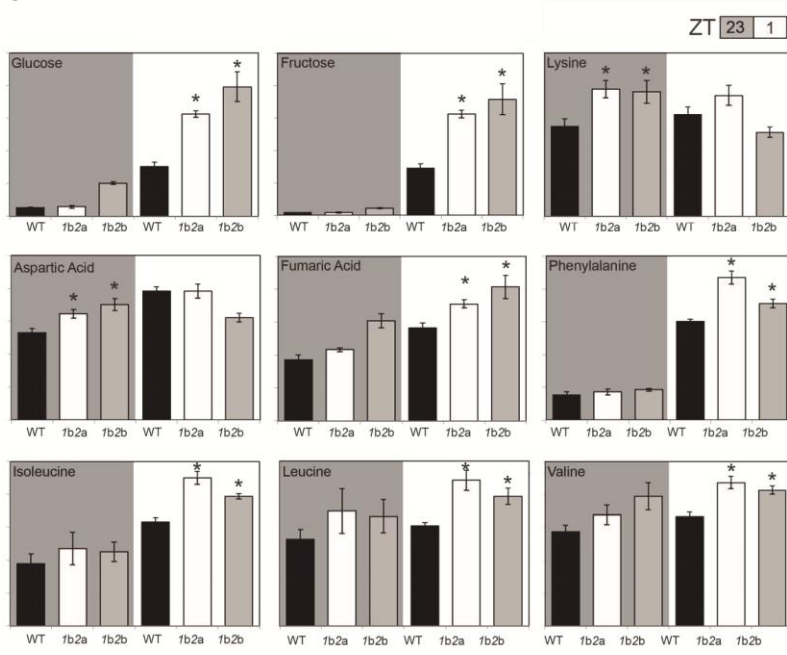
- (a,b) Parameters related to rosette growth (a) and flowerig time (b) in WT plants and two independent *35S:CYTC* lines grown under LD conditions. DAS: days after sowing. The bars represent the mean $\pm$ SD of 12 plants from each genotype. Asterisks indicate significant differences ( $P < 0.01$ ) with WT plants according to LSD Fisher tests.
- (c) Representative images of WT and *35S:CYTC* plants.
- (d) RGA protein levels in WT and two independent *35S:CYTC* lines analyzed by Western blot.

(e) CYTc protein levels in WT, *35S:CYTC* and *ga1-3* plants and three different homozygous plants obtained after crossing *35S:CYTC* line 1 with *ga1-3* plants.

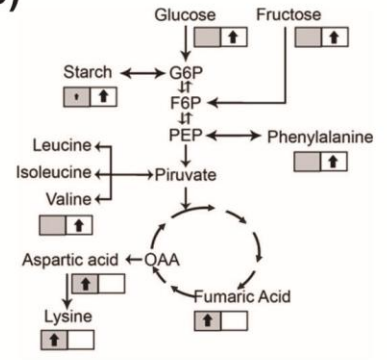
(f) Phenotype of plants under control conditions (upper panel) or after treatment with GA as described in the legend of Figure 4 (lower panel). The images are representative of experiments performed with at least five different plants from each line.



(a)



(b)



(c)

